

# Modelling and simulation of flow and agglomeration in deep veins valves using discrete multi physics

Ariane, M; Wen, W; Vigolo, D; Brill, A; Nash, F G B; Barigou, M; Alexiadis, A

DOI:

[10.1016/j.compbiomed.2017.07.020](https://doi.org/10.1016/j.compbiomed.2017.07.020)

License:

Creative Commons: Attribution-NonCommercial-NoDerivs (CC BY-NC-ND)

*Document Version*

Peer reviewed version

*Citation for published version (Harvard):*

Ariane, M, Wen, W, Vigolo, D, Brill, A, Nash, FGB, Barigou, M & Alexiadis, A 2017, 'Modelling and simulation of flow and agglomeration in deep veins valves using discrete multi physics', *Computers in Biology and Medicine*, vol. 89, pp. 96-103. <https://doi.org/10.1016/j.compbiomed.2017.07.020>

[Link to publication on Research at Birmingham portal](#)

## General rights

Unless a licence is specified above, all rights (including copyright and moral rights) in this document are retained by the authors and/or the copyright holders. The express permission of the copyright holder must be obtained for any use of this material other than for purposes permitted by law.

- Users may freely distribute the URL that is used to identify this publication.
- Users may download and/or print one copy of the publication from the University of Birmingham research portal for the purpose of private study or non-commercial research.
- User may use extracts from the document in line with the concept of 'fair dealing' under the Copyright, Designs and Patents Act 1988 (?)
- Users may not further distribute the material nor use it for the purposes of commercial gain.

Where a licence is displayed above, please note the terms and conditions of the licence govern your use of this document.

When citing, please reference the published version.

## Take down policy

While the University of Birmingham exercises care and attention in making items available there are rare occasions when an item has been uploaded in error or has been deemed to be commercially or otherwise sensitive.

If you believe that this is the case for this document, please contact [UBIRA@lists.bham.ac.uk](mailto:UBIRA@lists.bham.ac.uk) providing details and we will remove access to the work immediately and investigate.

# Accepted Manuscript

Modelling and simulation of flow and agglomeration in deep veins valves using discrete multi physics

M. Ariane, W. Wen, D. Vigolo, A. Brill, F.G.B. Nash, M. Barigou, A. Alexiadis



PII: S0010-4825(17)30244-5

DOI: [10.1016/j.compbiomed.2017.07.020](https://doi.org/10.1016/j.compbiomed.2017.07.020)

Reference: CBM 2731

To appear in: *Computers in Biology and Medicine*

Received Date: 8 May 2017

Revised Date: 10 July 2017

Accepted Date: 28 July 2017

Please cite this article as: M. Ariane, W. Wen, D. Vigolo, A. Brill, F.G.B. Nash, M. Barigou, A. Alexiadis, Modelling and simulation of flow and agglomeration in deep veins valves using discrete multi physics, *Computers in Biology and Medicine* (2017), doi: 10.1016/j.compbiomed.2017.07.020.

This is a PDF file of an unedited manuscript that has been accepted for publication. As a service to our customers we are providing this early version of the manuscript. The manuscript will undergo copyediting, typesetting, and review of the resulting proof before it is published in its final form. Please note that during the production process errors may be discovered which could affect the content, and all legal disclaimers that apply to the journal pertain.

**Modelling and simulation of flow and agglomeration in deep veins valves using Discrete Multi Physics.**

M. Ariane<sup>a,\*</sup>, W. Wen<sup>a</sup>, D. Vigolo<sup>a</sup>, A. Brill<sup>b</sup>, F. G.B Nash<sup>b</sup>, M. Barigou<sup>a</sup>, A. Alexiadis<sup>a,\*</sup>

<sup>a</sup> School of Chemical Engineering, University of Birmingham, Birmingham, United Kingdom

<sup>b</sup> Institute of Cardiovascular Sciences, University of Birmingham, Birmingham, United Kingdom

**Abstract**

The hemodynamics in flexible deep veins valves is modelled by means of discrete multi-physics and an agglomeration algorithm is implemented to account for blood accrual in the flow. Computer simulations of a number of valves typologies are carried out. The results show that the rigidity and the length of the valve leaflets play a crucial role on both mechanical stress and stagnation in the flow. Rigid and short membranes may be inefficient in preventing blood reflux, but reduce the volume of stagnant blood potentially lowering the chances of thrombosis. Additionally, we also show that in venous valves, cell agglomeration is driven by stagnation rather than mechanical stress.

**Keywords:** Discrete Multi-Physics, Smoothed Particle Hydrodynamics, biological venous valve, Clot, Deep Venous Thrombosis.

## 1. Introduction

Deep venous thrombosis (DVT) is a dangerous and painful condition in which blood thrombi form in deep veins. Such thrombi contain blood cells (including red blood cells and platelets) within a mesh of coagulated protein which is predominantly fibrin. If one of these aggregates detaches from the vein, it can reach the lungs resulting in a life-threatening complication known as pulmonary embolism (PE). In the UK alone, DVT and PE (designated together as venous thromboembolism, VTE) cause an estimated 25,000 deaths annually which exceeds the number of deaths from breast cancer, AIDS and road traffic accidents combined (Hunt 2009).

One of the factors exacerbating DVT is prolonged immobility (e.g. bed ridden after surgery, limb paralysis and long-haul flights), where the insufficient efficacy of the muscle pump, which normally assists blood flow through the leg veins, leads to sluggish flow. Stasis and low flow states are classically associated with a high probability of thrombus formation (Reitsma et al., 2012). Because of this, it is likely that specific flow patterns in veins, especially around the valve flaps, can play a fundamental role in the formation of thrombi (Bovill and van der Vliet, 2011). Since hydrodynamics is affected by the valve characteristics, the valve characteristics can also affect thrombus agglomeration but the actual mechanisms remain unclear.

Moreover, once a person has developed DVT and has been successfully treated, he or she is likely to develop other thrombus in the future, suggesting that the person's specific valve geometry or flexibility may also contribute to the solid blood formation.

By providing hydrodynamic information of the blood flow around the valve, computer simulations can improve our understanding of the link between fluid dynamics and DVT. Computational blood dynamics has been widely and successfully used for cardiac valves (e.g. De Hart et al., 2000; Fenlon and David, 2001; Van Loon et al., 2004; Buxton and Clarke, 2006; Watton et al., 2007; Van Loon 2010; Astorino et al., 2012; Espino et al., 2012; Bahraseman et al., 2014; Al-Azawy et al., 2015; Borazjani 2015; Halevi et al., 2015; Kamensky et al., 2015; Marom 2015; Miandehi et al., 2015; Bavo et al., 2016), but with a few exceptions so far little attention has been given to venous valves (e.g. Wijeratne and Hoo 2008; Keijsers et al., 2015). In the majority of the venous valve simulations, the valve is fixed and the complex interaction between the flow and the moving leaflets is lost. Recently, flexible structures were investigated with the Fluid Structure Interaction (FSI) method (Simao et al., 2016). Nevertheless, analyses remain often limited to few cycles or implemented with one symmetrical leaflet. One of the reasons is related to the intrinsic difficulty of the FSI to simulate the leaflets' contact at the end of the closing phase. A few studies (e.g. Van Loon et al. 2010, Kamensky et al. 2015) used additional contact algorithms to account for the mechanical contact of leaflets. However, the implementation of these algorithms is complex and the frequency of the re-meshing close to the contact point remains an issue.

In this work, we use the Discrete Multi-Physics (DMP) approach developed in Alexiadis (2015) to model both the fluid dynamics and the flexible leaflets. This approach was previously used for cardiac valves (Ariane et al., 2017). In this previous paper, based on both dimensionless analysis and direct numerical simulations, we have shown that size and rigidity of the leaflets, together with inlet velocity, are key parameters and have determined which factors most affect the hydrodynamics around

the valve. For comparison, we focus on these parameters in this study, to specific flow patterns and stress profiles in a venous valve system using the DMP approach.

Other advantages of the approach proposed here is that, contrary to FSI simulation, it can account for a complete valve closure without the use of a stabilisation algorithm.

Finally, using DMP gives the possibility of introducing an agglomeration algorithm that transforms a portion of the liquid into a solid. Other studies (e.g. Simao et al., 2016) simulated cell aggregates by tweaking the viscosity of the liquid, but with the method proposed here we can form actual solid structures within the liquid phase. By introducing the agglomeration algorithm, we identify among the regions where thrombi are most likely to form and which have the highest growth probability.

## 2. Modelling

### 2.1. Modelling approach

The DMP modelling technique used in this work is based on the so-called discrete multi-hybrid system (DMHS). In the DMHS model, the liquid is represented by Smoothed Particle Hydrodynamics (SPH) particles (Monaghan 1994; Morris et al., 1997; Liu and Liu 2003), while the solid structure is divided into many notional particles linked by computational springs (to model the elastic modulus of the solid), computational hinges (to model the flexural modulus) and computational dashpots (to model the viscous material behaviour). Mathematically, this is similar to the treatment of molecular bonds used in Molecular Dynamic (MD) simulations. In the original paper where the DMHS was first proposed (Alexiadis 2014), this part of the model was referred to as Coarse Grained Molecular Dynamics (CGMD) to highlight its MD origin. Here we prefer the term Mass-Spring Model (MSM) as the scales involved are macroscopic. Readers can refer to Appendix A for details and to (Ariane et al., 2017) for application of this methodology to biological valves.

### 2.2. Geometry

In this study, we use a 2D schematic representation of the leg venous valve (Wijeratne and Hoo 2008) as illustrated in Fig. 1. The channel radius is  $Z = 0.004$  m, the radius of the valve chamber is  $R = 0.007$  m and its length is  $Y = 0.04$  m. Three different lengths  $L$  of the membrane are studied: long (0.0256 m), medium (0.0175 m) and short (0.01 m). In order to distinguish different parts of the geometry, we refer to the region between

the two leaflets as the ‘opening region’ and to the two regions between the wall and the leaflet as ‘sinus regions’. Fig. 1 shows the location of the opening region and one of the two sinus regions (the other is symmetric and located above the upper leaflet).

**Fig. 1.** Illustration of the venous valve 2D geometry and particle representation.

The leaflets are represented by (solid) MSM particles joined together by springs and hinges (fig. 1) as discussed in Appendix A. SPH particles are used for the fluid and stationary (solid) particles for the walls. Three layers of particles are used for the channel and two for each leaflet.

There are two types of parameters required for the simulations: model parameters and simulation parameters. The first group consists of internal parameters used by the SPH and MSM solvers (Table 2); the second refers to the operative conditions detailed below.

## 2.3 Simulation conditions

The Young’s modulus  $E$  and the flexural modulus  $F$  of the membrane are the results of the MSM particles joined together by numerical springs and hinges. The relation between the spring ( $k_b$ ) and hinge ( $k_a$ ) constants and the actual Young’s modulus and the flexural modulus is given in Ariane et al. (2017). A viscous coefficient is added to the MSM springs to confer viscoelastic properties to the membrane as in a Kelvin–Voigt material.

Periodic boundary conditions are used at the inlet/outlet and we implement the same pulsatile flow (purely oscillatory) used by (Wijeratne and Hoo 2008) and imposing to each liquid particle the acceleration  $g$  as shown in equation 1



$$g = g_0 \sin(2\pi ft), \quad (1)$$

with amplitude  $g_0$  (given in Table 1), time  $t$  and oscillation frequency  $f = 1/T$  (with  $T$  the period oscillation). We use equation 1 as a simple means of forcing alternating flow in the valve, but the real oscillation is not sinusoidal and the frequency is not constant. We chose  $T = 4$  s, which is long enough to ensure full closure. Here we limit the total time of calculation with 4 full cycles (opening and closing) which correspond to 16 s. Previous work (Wijeratne and Hoo 2008) used  $T = 3$  s and simulated only one full cycle. When the muscles contract, the blood within the veins is compressed and the valve opens; when the muscles dilate, the valve closes preventing backward flow. The blood velocity depends on the force of the muscle contraction and, in general, it is related to the level of physical activity of a specific person. In order to account for three levels of physical activity, we take into account three values of  $g_0$  ( $0.1 \text{ m s}^{-2}$ ,  $0.25 \text{ m s}^{-2}$  and  $0.4 \text{ m s}^{-2}$ ), which result in three different flows with maximum velocities in the inlet channel of  $0.03 \text{ m s}^{-1}$  (low physical activity),  $0.07 \text{ m s}^{-1}$  (intermediate case),  $0.13 \text{ m s}^{-1}$  (high level of physical activity) respectively. The low velocity is from (Simao et al., 2016), the intermediate velocity is from (Wijeratne and Hoo 2008) and we include the third highest velocity to account for high levels of physical activity. In all cases, the flow is laminar.

The length and the flexibility of the membrane vary from person to person (Mühlberger et al., 2008; Moore et al., 2011). In order to investigate a variety of individual variations, we consider three membrane lengths (0.0256 m, 0.0175 m, and 0.01 m). The longest length is from (Wijeratne and Hoo 2008) and the shortest length is chosen as the minimum size allowing a complete closure of the leaflets. Regarding the flexibility and

the stiffness, in our previous paper (Ariane et al. 2017), the literature review for the aortic valve has shown that the membrane has three dynamic regimes based on the membrane stiffness (Bavo et al. 2016; Ledesma et al. 2014; De Hart et Al. 2000; Van Loon et al. 2006). In the simulation, we vary the stiffness of the valve according to these regimes (see Table 1).

**Table 1.** List of simulations with fluid velocities and membrane parameters.

<b>Variation of the membrane length and the velocity with <math>k_a = 0.01J</math></b>		
Length of the membrane $L [m]$	$V [m s^{-1}]$	Designation
Short $L = 0.01 m$	0.03	L0.01/V0.03/ $k_a0.01$
	0.07	L0.01/V0.07/ $k_a0.01$
	0.13	L0.01/V0.13/ $k_a0.01$ .
Medium $L = 0.0175 m$	0.03	L0.0175/V0.03/ $k_a0.01$
	0.07	L0.0175/V0.07/ $k_a0.01$
	0.13	L0.0175/V0.13/ $k_a0.01$ .
Long $L = 0.0256 m$	0.03	L0.0256/V0.03/ $k_a0.01$
	0.07	L0.0256/V0.07/ $k_a0.01$
	0.13	L0.0256/V0.13/ $k_a0.01$
<b>Variation of the membrane flexibility with <math>L = 0.0256m</math> and <math>V = 0.07 m s^{-1}</math></b>		
Angular coefficient $k_a [J]$		Designation
0.0001		L0.0256/V0.07/ $k_a0.0001$
0.002		L0.0256/V0.07/ $k_a0.002$
0.005		L0.0256/V0.07/ $k_a0.005$
0.02		L0.0256/V0.07/ $k_a0.02$
0.05		L0.0256/V0.07/ $k_a0.05$

## 2.4 Agglomeration algorithm

In order to understand the agglomeration dynamics, we introduce in the model the agglomeration algorithm developed in Ariane et al. (2017) (a brief overview of the method can be found in Appendix B). At this stage, our focus is to understand if *hydrodynamics alone* favours agglomeration at different locations. The actual biochemical process of thrombus formation is an extremely complex phenomenon (e.g. Panteleev et al., 2015) and it is beyond the scope of this article.

Specific particle points are used as agglomeration seeds. The algorithm every  $N$  time-steps checks all the fluid particles at a distance  $R_{\text{MAX}}$  from the seeds and, with a certain probability  $P$ , transforms some of these particles into solid agglomerate-particles.

In the simulations, the values of  $N$ ,  $R_{\text{MAX}}$  and  $P$  are given in Table 2. These values do not correspond to the real time-scale of agglomeration but were chosen in order to accelerate agglomeration and to observe significant growth in few cycles. Since our goal is to determine where agglomeration is more likely, this ‘accrual acceleration’ does not affect the validity of the results, as long as the timescale of agglomeration is longer than the timescale of the flow.

169 **Table 2.** Model parameters used in the simulations.

SPH (eq.s A.5–A.7)	
Parameter	Value
Number of SPH wall particles (3 layers)	5360
Number of SPH valve particles (2 layers)	(1) 1026, (2) 702, (3) 402
Number of SPH fluid particles	(1) 89592, (2) 89726, (3) 90012
Mass of each particle (fluid)	$1.05 \cdot 10^{-5}$ kg
Mass of each particle (wall and valve)	$2 \cdot 10^{-5}$ kg
Initial distance among particles $\Delta r$	$1 \cdot 10^{-4}$ m
Smoothing length $h$	$2.5 \cdot 10^{-4}$ m
Artificial sound speed $c_0$	$10 \text{ m s}^{-1}$
Density $\rho_0$	$1056 \text{ kg m}^{-3}$
Time step $\Delta t$	$10^{-7}$ s
CGMD (eq.s A.10–A.11)	
Parameter	Value
Angular coefficient $k_a$	See Table 1
Hookian coefficient $k_b$	$1 \cdot 10^6 \text{ J m}^{-2}$
Viscous damping coefficient $k_v$	$0.01 \text{ kg s}^{-1}$
Equilibrium distance $r_0$	$1 \cdot 10^{-4}$ m
Equilibrium angle $\theta_0$	$\pi/2$ rad
BOUNDARIES (eq. A.15)	
Constant $K$	$4 \cdot 10^{-4} \text{ J}$
Repulsive radius $r^*$	$1 \cdot 10^{-4}$ m
SOLID FORMATION (Section Formation of solid aggregates)	
Number of time step for solid formation $N$	$0.5 \cdot 10^6$ s
$R_{\max}$	$2.5 \cdot 10^{-4}$ m
Agglomeration probability $P$	50 %
Max bonds per solid particle	4
(a) long, (b) medium, (c) short membrane	

170

171

### 3. Results and discussion

#### 3.1 Stress and residence time

According to (Simao et Al., 2016), causes of DVT among young people remain unknown in most of half of the cases. When the origin of DVT is known, thrombus initiation is often associated with blood coagulability, changes in the vessel wall or immobility (Esmon 2009). In the case of immobility, low velocity and high residence time are the most causes of blood aggregation (Menichini et Al. 2016, Bovill et Al. 2011). Although, shear stress can also play a role in platelet aggregation and activation. In fact, components of the coagulation cascade and platelets can be activated in all shear stresses, just mechanisms will be different. For instance, at low shear stress, platelets adhere to fibrinogen, whereas at high shear stress to von Willebrand factor (Ikeda et al., 1991). Likewise, abnormal shear stress distribution can initiate and accelerate the formation of thrombi (Hou et Al., 2015). In the arterial setting, high stress could be an activator of platelet aggregation (Zhang et al., 2002). However, arterial and venous thrombi are structurally different. In arteries, high shear may induce platelet activation and formation of what is sometimes called *white thrombi* with few red cells in it. In veins, the thrombus is red with many red cells trapped in coagulated proteins. In this case, coagulation seems to be the dominant process, suggesting a slower, time dependant, accrual.

The following discussion focuses on both mechanical stress and residence time, to account for the two factors that are most generally related to thrombus formation (Zhang et al., 2002).

### 3.1.1 Mechanical stress

Our DVT calculations show that shear stress is high only in the opening region and almost negligible everywhere else (Fig. 2a). Clinical experience, however, indicates that thrombi do not form in the opening region, where shear stress is high, but rather in the sinus region (Bovill and van der Vliet 2011) where it is at its lowest (Ju et al., 2016). These observations suggest that *total mechanical stress* ( $T_{tot}$ ), rather than shear stress ( $T_{shear}$ ) should be investigated and our results show that, in this case,  $T_{tot}$  is high on both sides of the membrane (Fig. 2b).

In a fluid, the *total mechanical stress* (or total mechanical force) is the sum of shear stress (or viscous forces), inlet pressure (or pressure force,  $P_{tot}$ ) and gravity (or Body force, ignored here). Fig. 2c shows the pressure profile and indicates that the higher *total mechanical stress* on the membrane cannot be justified by pressure alone. When a solid body moves in the fluid (acceleration or deceleration), it generates additional forces (virtual mass force) that simultaneously move the volume of the surrounding fluid. These inertial forces so-called *added forces* explain the higher  $T_{tot}$  on the membrane in the sinus region.

**Fig. 2.** Shear stress (a), total mechanical stress (b), pressure (c), and velocity magnitude (d) for  $L0.0256/V0.03/k_a0.01$

### 3.1.2. Residence time in the sinus

In Lagrangian approach, displacement is used as a proxy for residence time and the following discussion is based on this parameter instead of residence time.

As shown in Fig. 2d, the velocity in the sinus region is low compared to that of the opening region; as a consequence, the residence time of fluid particles in this region is higher. Fig. 3 illustrates this point. We highlight the particles initially in the sinus in blue and we track their position during the simulation. At the end of four cycles, a fraction of the particles has left the sinus, while the rest remains confined in this region. In Fig. 3, the particles are coloured according to their *displacement*, defined as the distance travelled by each particle during the simulation. Blue particles do not move very much and are substantially stagnant; red particles have higher velocity and show higher displacement.

**Fig. 3.** Simulation snapshots illustrating the fluid motion of the particles initially in the sinus at different times (beginning of each new cycle): for  $L0.0256/V0.03/k_a0.01$ ; particles coloured according to their displacement.

In the sinus, we can identify two areas of high fluid displacement. The first (called ‘mixing region’ in Fig. 3) corresponds to the recirculation region created by the backflow (Fig. 4). The second (called ‘compression region’ in Fig. 3) is below the membrane and corresponds to the part of the fluid displaced by the oscillating movement of the membrane. There is a fundamental difference between the two regions. While in the mixing region the fluid particles are actually moved out of the sinus by the backflow, in the compression region the particle only oscillates around the same point due to the alternate motion of the membrane.

**Fig. 4.** Velocity profile in the sinus area (vectors) for  $L0.0256/V0.03/k_a0.01$ .

Despite the fact that both regions show high displacement, the actual residence time is high only in the compression region.

Displacement alone, therefore, is not enough to distinguish between regions of low and high residence time. In order to account for this, in the next section, we introduce the time-averaged displacement as a more accurate proxy for the residence time.

### 3.2. Parametric study

In this section, we investigate how  $T_{tot}$  and displacement are affected by (i) membrane flexibility, (ii) leaflet length and (iii) level of physical activity (fluid velocity). According to our simulations, all of these three parameters are particularly significant for the performance of the valve. Comparing the effect of these parameters among different setups, however, is not straightforward because it changes in space and time. To compare results with respect to the same reference point, we identify the fluid particle in the sinus region with the highest mechanical stress and for every setup we measure stress and displacement at this location. In this way, we carry out all our measurements at the same relative position. However, as indicated in Fig. 5a and 5b, displacement and  $T_{tot}$  also change with time. To account for this, in the case of displacement (Fig. 5a), we use the time-average instead of the instantaneous displacement. In the case of  $T_{tot}$  (Fig. 5b), we use the maximal rather than the average stress because agglomeration is more affected by the peak of the stress rather than its average.

**Fig. 5.** Time evolution of the local fluid displacement (a) and total mechanical stress magnitude (b) for the particle of maximal stress (L0.0256/V0.03/ $k_a$ 0.01).



We can also quantify how both these parameters oscillate with time by calculating their standard deviation; in the subsequent Figs, the error bars indicate the standard deviation.

### 3.2.1. Effect of membrane flexibility

The flexibility of the membrane depends on its flexural modulus. In Ariane et al. (2017) we showed that the flexural modulus is mostly affected by the  $k_a$ , for this reason, in this section we focus on how time-averaged displacement and maximal stress vary with this parameter.

In Fig. 6, both average displacement and  $T_{tot}$  decrease as the membrane flexibility increases to a value  $k_a = 0.02$  J because mechanical deformation is lower for rigid membranes. However, the displacement for very rigid membranes ( $k_a = 0.05$  J) increases. The reason for this can be understood by comparing Fig. 7a and 7b: at  $k_a = 0.05$  J, the leaflets maintain a straight profile during the closure phase (Fig. 7a), while at  $k_a = 0.02$  J they bend under the flow (Fig. 7b). When the leaflets bend, they partially shield the sinus region from the backflow and reduce the velocity (and therefore the displacement). Conversely, very flexible membranes ( $k_a < 0.005$  J) highly deform and fluctuate under the flow (Fig. 7c). This explains the higher standard deviation in Fig. 6 and the irregular profile of Fig. 6b for  $k_a < 0.005$  J.

**Fig. 6.** Time-averaged displacement (a) and total mechanical stress (b) versus  $k_a$  (valve flexibility) for cases:  $L = 0.0256$  m,  $V = 0.07$  m s<sup>-1</sup> and  $k_a$  from 0.0001J to 0.05J.

**Fig. 7.** Simulation snapshots illustrating the fluid motion of the particles initially in the sinus for long valve,  $V = 0.07$  m s<sup>-1</sup> and three flexibilities: (a)  $k_a = 0.05$  J, (b)  $k_a = 0.02$  J, and (c)  $k_a = 0.0001$  J, particles coloured according to their displacement.

### 3.2.2. *Effect of membrane length and inlet velocity*

Fig. 8 shows the effect of the inlet velocity on the displacement and stress for three membrane sizes. For medium or long membranes, as expected, higher velocities are associated with higher stress and displacement. The short membrane, however, behaves differently.

**Fig. 8.** Evolution of displacement (a) and total mechanical stress magnitude (b) with the maximum inlet velocity.

Contrary to the medium and long membrane (see Fig. 2), in short membranes, the highest stress (see Fig. 9) is located at the tip rather than the middle of the valve. At the tip, the motion of the particles depends on the hydrodynamics at the opening region rather than that at the sinus region and, therefore, they are easily transported away by the flow and the displacement increases significantly.

**Fig. 9.** Total mechanical stress (a), velocity magnitude (b), vector velocity (c), and displacement (d) in the short valve case for  $L0.01/V0.07/k_a0.01$ .

### 3.3. Agglomeration

The main physical parameters that affect agglomeration are the residence time and mechanical stress. The simulations highlight two key locations: one at the sinus side of the membrane, where stress is the highest (point  $P_1$  in Fig. 10), and the other at the valve/wall connection where the residence time is the highest (point  $P_2$  in Fig. 10).

The higher mechanical stress at  $P_1$  pushes particles closer, increasing the number of particles inside  $R_{MAX}$ ; however, because the velocity is higher, these particles remain

inside  $R_{MAX}$  only for a short time. At  $P_2$ , the opposite happens: the mechanical stress is lower, but also, because the velocity is low (and, therefore, the residence time is high) and the particles remain inside  $R_{MAX}$  for longer.

High stresses and high velocities, therefore, have opposite effects on agglomeration. Fig. 10 shows faster growth at  $P_2$ , suggesting that residence time may be more important for aggregation propagation in the venous valve than mechanical stress.

**Fig. 10.** Solid aggregates in the sinus region at two different times for  
L0.0175/V0.07/ $k_a$ 0.01.

## Conclusions

This article presents a discrete multi-physics model for both blood dynamics and leaflets mechanics of a leg venous valve. In the simulations, we focused on mechanical stress and flow stagnation (high residence time) in the sinus region because these two factors have been linked to the onset of blood solid formation. The model is subsequently coupled with an agglomeration algorithm to account for the formation and propagation of solid aggregates in the flow.

The results show that the flexibility and the length of the membrane play a crucial role in both stress and flow stagnation. Rigid membranes do not close completely and, therefore, they may be inefficient in preventing blood reflux. However, they also allow for a larger flow exchange between the sinus region and the central flow reducing stagnation and, potentially, lowering the chances of thrombosis. Similarly, short membranes reduce the volume of the sinus region, which also decreases stagnation.

We also focused on the issue in venous valves and whether it is mechanical stress or stagnation that favours cell agglomeration which may lead to thrombosis.

In order to compare the role of these two factors, we identified the location in the sinus with the highest stress and that with the highest stagnation. We placed an agglomeration seed in each of these two locations and implemented our agglomeration algorithm.

The growth of the agglomerate at the point of maximum stagnation was considerably higher than that at the point of maximal stress. This implies that, in the case of the venous valve, stagnation can be more important than mechanical stress in thrombus formation and propagation.

This result, combined with the fact that membrane flexibility and length determine the level of stagnation in the sinus, highlights the potential for personalised diagnostics in the fight against deep venous thrombosis. In principle, length and stiffness could be evaluated in clinical setting using existing diagnostic methods. Currently, they are not evaluated, but based on our results, if they were added, in the future, to the toolkit of physicians they could, potentially, help predicting the likelihood of DVT.

These data, in fact could be introduced into our discrete multi physics model to predict, for that particular valve, the location of maximum stagnation and provide information that, potentially, could be converted into a probability of thrombus formation for a specific individual.

## Acknowledgements

This work was supported by the Engineering and Physical Sciences Research Council (EPSRC) grant number: EP/N033698/1.

## Supporting Information

A Appendix

B Appendix

## References

- Al-Azawy, M. G., A. Turan and A. Revell (2015). "Assessment of turbulence models for pulsatile flow inside a heart pump." *Computer Methods in Biomechanics and Biomedical Engineering*: 1-15.
- Alexiadis, A. (2014). "A smoothed particle hydrodynamics and coarse-grained molecular dynamics hybrid technique for modelling elastic particles and breakable capsules under various flow conditions." *International Journal for Numerical Methods in Engineering* **100**(10): 713-719.
- Alexiadis, A. (2015). "The Discrete Multi-Hybrid System for the Simulation of Solid-Liquid Flows." *Plos One* **10**(5).
- Ariane, M., M. H. Allouche, M. Bussone, F. Giacosa, F. Bernard, M. Barigou and A. Alexiadis (2017). "Discrete multi-physics: A mesh-free model of blood flow in flexible biological valve including solid aggregate formation." *Plos One* **12**(4).
- Astorino, M., J. Hamers, S. C. Shadden and J.-F. Gerbeau (2012). "A robust and efficient valve model based on resistive immersed surfaces." *International Journal for Numerical Methods in Biomedical Engineering* **28**(9): 937-959.
- Bahraseman, H. G., K. Hassani, A. Khosravi, M. Navidbakhsh, D. M. Espino, N. Fatourae and D. Kazemi-Saleh (2014). "Combining numerical and clinical methods to assess aortic valve hemodynamics during exercise." *Perfusion-Uk* **29**(4): 340-350.

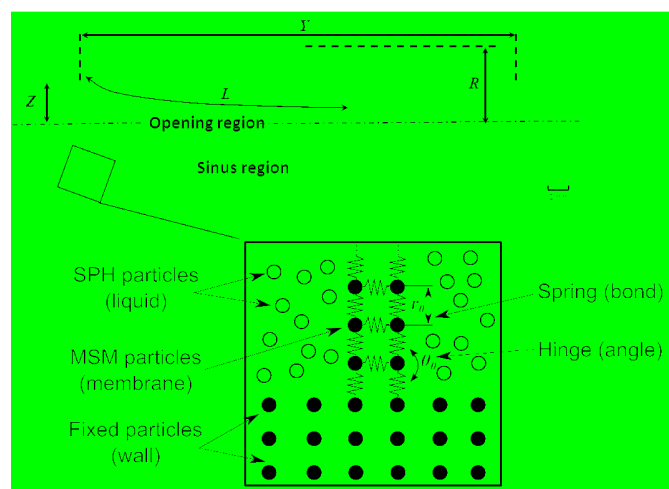
- Bavo, A. M., G. Rocatello, F. Iannaccone, J. Degroote, J. Vierendeels and P. Segers (2016). "Fluid-Structure Interaction Simulation of Prosthetic Aortic Valves: Comparison between Immersed Boundary and Arbitrary Lagrangian-Eulerian Techniques for the Mesh Representation." *Plos One* **11**(4).
- Borazjani, I. (2015). "A Review of Fluid-Structure Interaction Simulations of Prosthetic Heart Valves." **25**(1-2): 75-93.
- Bovill, E. G. and A. van der Vliet (2011). Venous Valvular Stasis-Associated Hypoxia and Thrombosis: What Is the Link? *Annual Review of Physiology*, Vol 73. D. Julius and D. E. Clapham. **73**: 527-545.
- Buxton, G. A. and N. Clarke (2006). "Computational phlebology: The simulation of a vein valve." *Journal of Biological Physics* **32**(6): 507-521.
- De Hart, J., G. W. M. Peters, P. J. G. Schreurs and F. P. T. Baaijens (2000). "A two-dimensional fluid-structure interaction model of the aortic valve." *Journal of Biomechanics* **33**(9): 1079-1088.
- Esmon, C. T. (2009). "Basic mechanisms and pathogenesis of venous thrombosis." *Blood Reviews* **23**(5): 225-229.
- Espino, D. M., D. E. T. Shepherd and D. W. L. Hukins (2012). "Evaluation of a transient, simultaneous, arbitrary Lagrange-Euler based multi-physics method for simulating the mitral heart valve." *Computer Methods in Biomechanics and Biomedical Engineering* **17**(4): 450-458.
- Fenlon, A. J. and T. David (2001). "Numerical models for the simulation of flexible artificial heart valves: part I--computational methods." *Computer methods in biomechanics and biomedical engineering* **4**(4): 323-339.

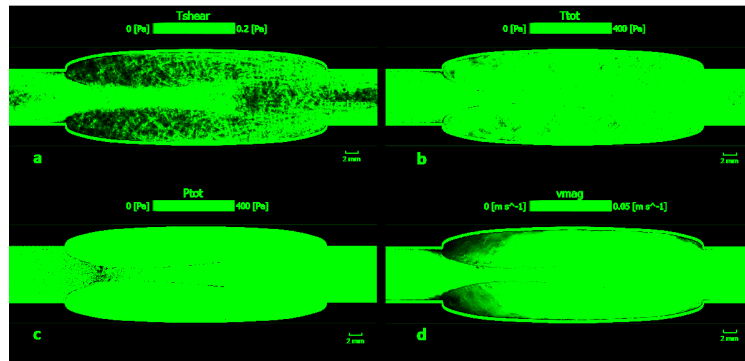
- Halevi, R., A. Hamdan, G. Marom, M. Mega, E. Raanani and R. Haj-Ali (2015).  
 "Progressive aortic valve calcification: Three-dimensional visualization and  
 biomechanical analysis." *Journal of Biomechanics* **48**(3): 489-497.
- Hou, X. Y., Sun, X., Shi, Y. T., Zhang, K. L. and Yao, J. T. (2015). "Simulation of the  
 formation mechanism of coronary thrombosis based on dem-cfd coupling." 2015 8th  
 International Conference on Biomedical Engineering and Informatics (Bmei): 24-28.
- Hunt, B. J. (2009). "The prevention of hospital-acquired venous thromboembolism in  
 the United Kingdom." *British Journal of Haematology* **144**(5): 642-652.
- Ikeda, Y., Handa, Kawano, M., Kamata, T., Murata, M., Araki, Y., Anbo, H., Kawai,  
 Y., Watanabe, K., Itagaki, I., Sakai, K., and Ruggeri, Z. M. (1991). "The role of  
 vonwillebrand-factor and fibrinogen in platelet-aggregation under varying shear-  
 stress." *Journal of Clinical Investigation* **87**(4): 1234-1240.
- Ju, L. N., Y. F. Chen, L. Z. Xue, X. P. Du and C. Zhu (2016). "Cooperative unfolding of  
 distinctive mechanoreceptor domains transduces force into signals." *eLife* **5**.
- Kamensky, D., M.-C. Hsu, D. Schillinger, J. A. Evans, A. Aggarwal, Y. Bazilevs, M. S.  
 Sacks and T. J. R. Hughes (2015). "An immersogeometric variational framework for  
 fluid–structure interaction: Application to bioprosthetic heart valves." *Computer  
 Methods in Applied Mechanics and Engineering* **284**: 1005-1053.
- Keijsers, J. M. T., C. A. D. Leguy, W. Huberts, A. J. Narracott, J. Rittweger and F. N.  
 van de Vosse (2015). "A 1D pulse wave propagation model of the hemodynamics of  
 calf muscle pump function." *International Journal for Numerical Methods in  
 Biomedical Engineering* **31**(7).
- Liu, G. R. and M. B. Liu, Eds. (2003). *Smoothed Particle Hydrodynamics: a meshfree  
 method*. Singapore, World Scientific Publishing Co. Pte. Ltd.

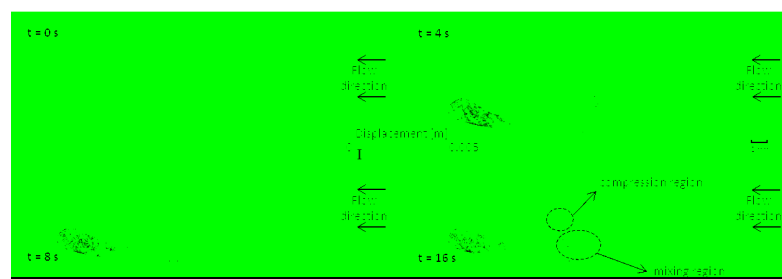
- 414 Marom, G. (2015). "Numerical Methods for Fluid–Structure Interaction Models of  
415 Aortic Valves." *Archives of Computational Methods in Engineering* **22**(4): 595-620.
- 416 Menichini, C., Cheng, Z., Gibbs, R. G. J. and Xu, X. Y. (2016). "Predicting false lumen  
417 thrombosis in patient-specific models of aortic dissection." *Journal of the Royal  
418 Society Interface* **13**(124).
- 419 Miandehi, E. E., M. H. Aazami, H. Niazmand, Y. Mesri, A. Deyranlou and S. Eslami  
420 (2015). "Clinical simulation of aortic valve: a narrative review." *Studies in health  
421 technology and informatics* **210**: 612-616.
- 422 Monaghan, J. J. (1994). "Simulating Free Surface Flows with SPH." *Journal of  
423 Computational Physics* **110**(2): 399-406.
- 424 Moore, H. M., M. Gohel and A. H. Davies (2011). "Number and location of venous  
425 valves within the popliteal and femoral veins - a review of the literature." *Journal of  
426 Anatomy* **219**(4): 439-443.
- 427 Morris, J. P., P. J. Fox and Y. Zhu (1997). "Modeling Low Reynolds Number  
428 Incompressible Flows Using SPH." *Journal of Computational Physics* **136**(1): 214-  
429 226.
- 430 Mühlberger, D., L. Morandini and E. Brenner (2008). "An anatomical study of femoral  
431 vein valves near the saphenofemoral junction." *Journal of Vascular Surgery* **48**(4):  
432 994-999.
- 433 Panteleev, M. A., N. M. Dashkevich and F. I. Ataullakhanov (2015). "Hemostasis and  
434 thrombosis beyond biochemistry: roles of geometry, flow and diffusion."  
435 *Thrombosis Research* **136**(4): 699-711.

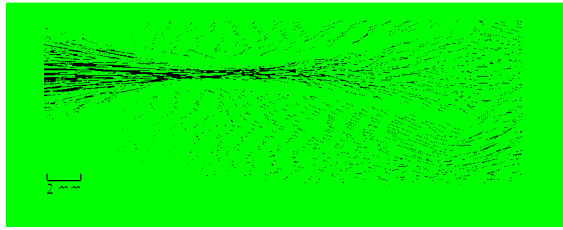


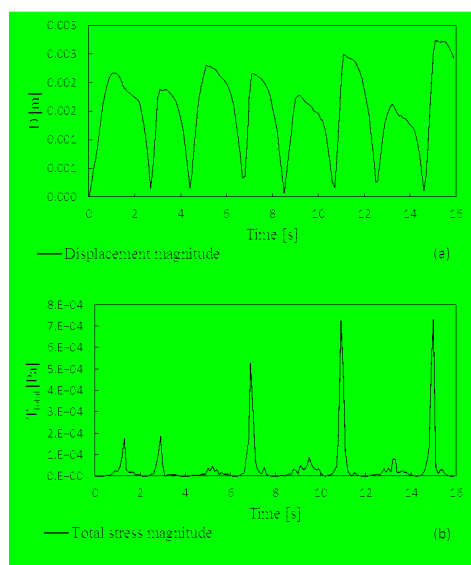
- Reitsma, P. H., H. H. Versteeg and S. Middeldorp (2012). "Mechanistic View of Risk Factors for Venous Thromboembolism." *Arteriosclerosis Thrombosis and Vascular Biology* **32**(3): 563-568.
- Simao, M., J. M. Ferreira, J. Mora-Rodriguez and H. M. Ramos (2016). "Identification of DVT diseases using numerical simulations." *Medical & Biological Engineering & Computing* **54**(10): 1591-1609.
- van Loon, R. (2010). "Towards computational modelling of aortic stenosis." *International Journal for Numerical Methods in Biomedical Engineering* **26**(3-4): 405-420.
- van Loon, R., P. D. Anderson, J. de Hart and F. P. T. Baaijens (2004). "A combined fictitious domain/adaptive meshing method for fluid-structure interaction in heart valves." *International Journal for Numerical Methods in Fluids* **46**(5): 533-544.
- Watton, P. N., X. Y. Luo, X. Wang, G. M. Bernacca, P. Molloy and D. J. Wheatley (2007). "Dynamic modelling of prosthetic chorded mitral valves using the immersed boundary method." *Journal of Biomechanics* **40**(3): 613-626.
- Wijeratne, N. S. and K. A. Hoo (2008). Numerical studies on the hemodynamics in the human vein and venous valve. 2008 American Control Conference, Vols 1-12. New York, Ieee: 147-152.
- Zhang, J.-n., A. L. Bergeron, Q. Yu, C. Sun, L. V. McIntire, J. A. López and J.-f. Dong (2002). "Platelet Aggregation and Activation under Complex Patterns of Shear Stress." *Thrombosis and Haemostasis* **88**(11): 817-821.

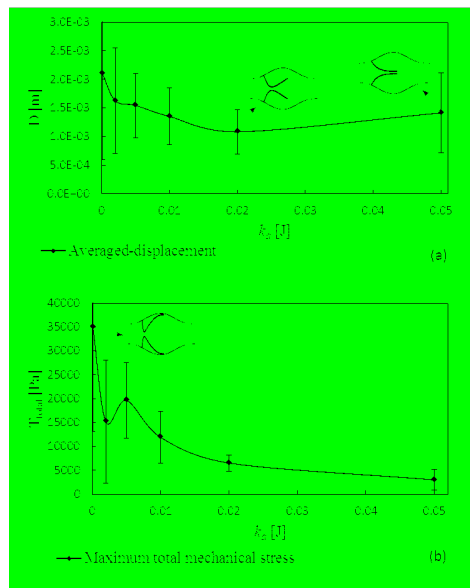


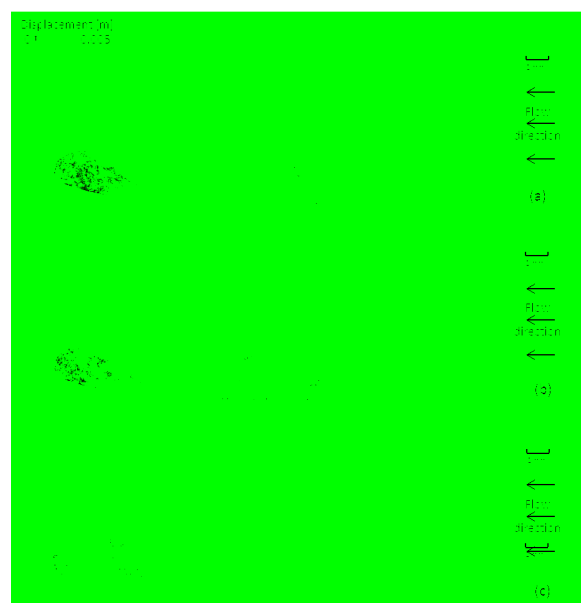




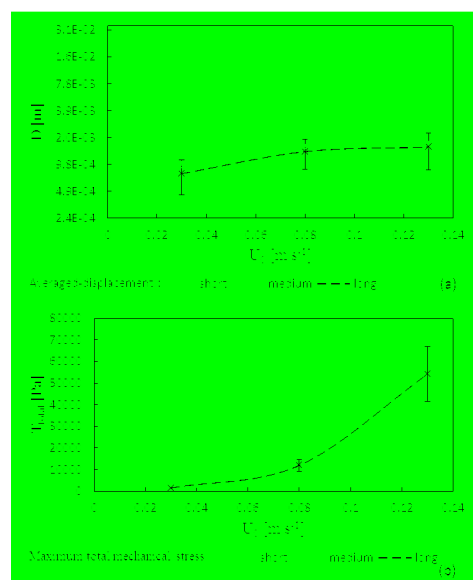


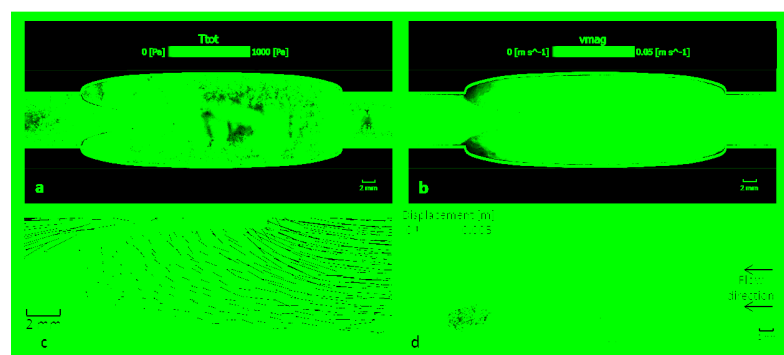


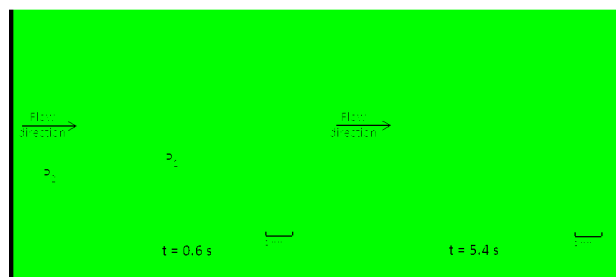












**Highlights:**

- Development of a discrete multi-physics model for both the blood dynamics and the leaflets mechanics in a leg venous valve.
- The model accounts for the hydrodynamics, the valve deformation with contact closure, and the solid aggregation at the same time.
- The key role of the flexibility and the length of the valve in both stress and flow stagnation are investigated.
- In venous valve, stagnation can be more important than stress in thrombus formation and propagation.